





PSEUDO JAHN-TELLER ORIGIN OF THE PROTON-TRANSFER ENERGY BARRIER IN THE HYDROGEN-BONDED [FHF]⁻ SYSTEM

Natalia Gorinchoy¹ ^{a*}, Iolanta Balan² ^a, Victor Polinger³ ^b, Isaak Bersuker⁴ ^{a,c}

^aInstitute of Chemistry, 3, Academiei str., Chisinau MD-2028, Republic of Moldova

^bUniversity of Washington, 109, Bagley Hall Box 351700 Seattle, WA 98195-1700, USA

^cUniversity of Texas at Austin, Austin, Texas 78712, USA

*email: ngorinchoy@yahoo.com; natalia.gorincioi@ichem.md

Abstract. The results of *ab initio* calculations of the adiabatic potential energy surfaces for the proton-bound [FHF]⁻ system at different F-F distances have been rationalized in the framework of the vibronic theory. It is shown that the instability of the symmetric $D_{\infty h}$ structure at increased F...F distances and the proton displacement to one of the fluorine atoms are due to the pseudo Jahn-Teller mixing of the ground electronic state $1^1\Sigma_g$ with the lowest excited state of $1^1\Sigma_u$ symmetry through the asymmetric σ_u vibrational mode.

Keywords: proton transfer, hydrogen bond, pseudo Jahn-Teller effect, potential energy surface, bifluoride anion.

Received: 20 April 2021/ Revised final: 17 May 2021/ Accepted: 21 May 2021

Introduction

The proton transfer process underlies many important chemical reactions such as reduction-oxidation interactions, high proton mobility in aqueous solutions, protons diffusion through membrane protein channels, *etc.* (see, for example, works [1-4] and references herein). A large number of experimental and theoretical works are devoted to the study of hydrogen-bonded molecular systems [5-7]. The bifluoride anion plays an especially important role in the study of the hydrogen bond. It was established both experimentally and by the benchmark quantum-chemical calculations that the [FHF]⁻ anion is linear and centrosymmetric in the gas phase, while in the crystal structures shifts of the proton from the mid-point are often observed [8-10]. The relationship between the F-H and F-F distances has been found and discussed [10]; in particular, it was shown that the longer the F-F distance, the greater the displacement of the H atom from the central position to one of the fluorine atoms.

Quantum-chemical calculations of such systems are mainly devoted to the determination of equilibrium geometric parameters and to the calculation of the adiabatic potential energy surfaces (APES) for the elaboration of pre-parametrized analytical potential models that could be used to simulate the proton transfer reaction [11-13].

On the other hand, it was shown earlier that the only reason of instability of the high-symmetry nuclear configurations and structural distortions of any molecular system in the nondegenerate state is the pseudo Jahn-Teller effect (PJTE), that is the vibronic mixing of considered state with the appropriate by symmetry excited states (see, for example, book [14] and reviews [15-17], and references therein). In systems with hydrogen bonds, a quantitative PJTE analysis was first used to study the origin of the hydrogen bond in the proton-bound ammonia dimer cation $N_2H_7^+$ [18], and for a number of protonated proton-centered water clusters [19]. In these papers, it was shown that this approach reveals many details that will prove useful for understanding hydrogen-bonded systems.

The main goal of the present work is to demonstrate that with increasing F-F distances, the instability of the central position of a proton in the [FHF]⁻ system and the appearance of a double-well adiabatic potential energy surface (APES) for proton transfer are due to the pseudo Jahn-Teller effect.

Method and computational details

The theory of the PJTE is well developed (see, *e.g.* [14,15]). In this approach the problem of the stability or instability of molecular nuclear configuration is reduced to the estimation of the

curvature K of the adiabatic potential energy surface (APES) of the system in the arbitrary direction Q at the high-symmetry configuration Q_0 for which the first derivatives are zero. In the second order perturbation theory with respect to small nuclear displacements Q the expression for K of any molecular system in its ground state $|\Psi_0\rangle$ can be written as:

$$K = K_0 + K_v \quad (1)$$

The first term in Eq.(1),

$$K_0 = \langle \Psi_0 | (\partial^2 H / \partial Q^2)_0 | \Psi_0 \rangle \quad (2)$$

is the so-called primary force constant. It determines the restoring force arising when the nuclei are displaced with respect to the “frozen” electronic distribution. The second term, which is always negative,

$$K_v = -2 \sum_n \frac{F_{0n}^2}{E_n - E_0} = -2 \sum_n \frac{|\langle \Psi_0 | (\partial H / \partial Q)_0 | \Psi_n \rangle|^2}{E_n - E_0} \quad (3)$$

is the vibronic contribution to the curvature K of the adiabatic potential arising from mixing of the ground $|\Psi_0\rangle$ and excited $|\Psi_n\rangle$ electronic states. In the Eqs.(2) and (3) H is the adiabatic electronic Hamiltonian of the system which includes all Coulomb interactions between electrons and nuclei, $|\Psi_i\rangle$ and E_i are, respectively, the electronic wave functions and the total energies of the ground and the excited states determined for the high-symmetry nuclear configuration, and $F_{0n} = \langle \Psi_0 | (\partial H / \partial Q)_0 | \Psi_n \rangle$ in Eq.(3) are the constants of the vibronic coupling of the ground Ψ_0 and the excited Ψ_n states. They are non-zero only if the product of irreducible representations of the wavefunctions Ψ_0 and Ψ_n contains the irreducible representation of the displacement Q .

It was proved analytically and confirmed by a series of numerical calculations [14,15,20-22] that for any molecular system $K_0 > 0$. Hence, a negative curvature K and, therefore, the structural instabilities and distortions can be achieved only

due to the negative vibronic coupling component K_v , and only if $|K_v| > K_0$. Thus, the value of K_0 , the energy gaps $\Delta_{0n} = E_n - E_0$ between the mixing states, and the vibronic coupling constants F_{0n} are the main parameters of the PJTE.

Direct calculation of the vibronic coupling matrix elements involved in the PJT models is rather difficult mathematically. In the present work the values of the PJTE parameters were estimated by fitting the *ab initio* calculated energy profiles (cross sections of the APES) of the [FHF]⁺ system along the instability coordinate σ_u (shifts of the proton from the mid-point of F...F distance) to the general formula, obtained from the vibronic theory. In the simplest case of the two-level PJTE problem when only one low-lying excited state contributes essentially to the instability of the ground state in the reference configuration, the roots of corresponding secular Eq.(4), where K_{01} and K_{02} are the primary force constants in the ground and the active excited state, respectively, and Δ_{12} is the energy gap between the mixing states, $\Delta_{12} = E_2 - E_1$.

Note, however, that in any polyatomic system there are always many excited states of relevant symmetry, albeit at large energy gaps $\Delta_{1n} = E_n - E_1$, which mix to the ground state by vibronic coupling. Their contribution to the PJTE problem can be taken into account by the second-order perturbation corrections p_1 and p_2 , which can be given in Eq.(5) [23-25], where F_{1n} and F_{2n} are the respective vibronic coupling constants between the states $|1\rangle$ and $|2\rangle$ and the high-energy excited states $|n\rangle$. They may be rather small, just lowering the curvature of the mixing states from K_{01} and K_{02} to $K_{01} - p_1$, and $K_{02} - p_2$, and not producing instability of the ground state. With such overdetermined values of K_{01} and K_{02} , Eq.(4) for fitting the parameters takes the form in Eq.(6).

At small Q the resulting values of the curvatures of the APES of the two states K_1 and K_2 that are coupled by the PJT interaction of the Q direction, in Eq.(7).

$$\varepsilon_{1,2} = \frac{1}{4}(K_{01} + K_{02})Q^2 + \frac{\Delta}{2} \mp \frac{1}{2} \sqrt{\left[\frac{1}{2}(K_{01} - K_{02})Q^2 - \Delta\right]^2 + 4F^2 Q^2} \quad (4)$$

$$-p_1 = -2 \sum_n \frac{|F_{1n}|^2}{E_n - E_1} \quad \text{and} \quad -p_2 = -2 \sum_n \frac{|F_{2n}|^2}{E_n - E_2} \quad (5)$$

$$\varepsilon_{1,2} = \frac{1}{4}(K_{01} - p_1 + K_{02} - p_2)Q^2 + \frac{\Delta}{2} \mp \frac{1}{2} \sqrt{\left[\frac{1}{2}(K_{01} - p_1 - K_{02} + p_2)Q^2 - \Delta_{12}\right]^2 + 4F_{12}^2 Q^2} \quad (6)$$

$$K_1 = (K_{01} - p_1) - 2F_{12}^2/\Delta \quad \text{and} \quad K_2 = (K_{02} - p_2) + 2F_{12}^2/\Delta \quad (7)$$

The geometry optimization and electronic structure calculations of $[\text{FHF}]^-$ systems at different F...F distances in their proton-centered $D_{\infty h}$ nuclear configurations were carried out in the frame of the RHF SCF method using the 6-31G* basis set [26]. The potential energy curves along the off-center proton displacement were calculated taking into consideration configuration interaction (CI) with single and double excitations (CISD). The active space of CI included five occupied and two lower unoccupied molecular orbitals. All calculations were performed by using the PC GAMESS version [27] of the GAMESS (US) QC package [28].

Results and discussion

The investigation started with the $[\text{FHF}]^-$ molecule from the reference configuration of $D_{\infty h}$ symmetry. The geometry optimization has shown that its equilibrium nuclear configuration corresponds to the symmetrical position of the H-atom, exactly in the middle of F...F distance (no imaginary frequency is observed). Calculated equilibrium F-F distance is equal to 2.24 Å. At the same time, the vibrational frequencies analysis of $[\text{FHF}]^-$ anions at increased F...F distances indicates the presence of one imaginary frequency (Table 1) corresponding to the low-symmetry σ_u -type distortion, which is mainly associated with the displacement of the proton towards one of the

fluorine atoms. This means that $D_{\infty h}$ configuration of these compounds is unstable with regard to the symmetrized σ_u displacements of its atoms. From Table 1 it can also be seen that with an increase in the F-F distance, the height and width of the barrier to proton transfer also increase.

The ground state wavefunction of the system belongs to the $^1\Sigma_g$ representation of the $D_{\infty h}$ symmetry point group; the valence electron configuration is $\dots(3\sigma_g)^2(1\pi_u)^4(1\pi_g)^4(3\sigma_u)^2(4\sigma_g)^0(5\sigma_g)^0(2\pi_u)^0(6\sigma_g)^0(2\pi_g)^0$. Some of these valence molecular orbitals are shown in Figure 1(a). According to the PJTE, excited states that produce the instability of the ground state should have the $^1\Sigma_u$ symmetry: $^1\Sigma_g \times ^1\Sigma_u = ^1\Sigma_u$. The first excited state $^1\Sigma_u$ is formed by one-electron excitation from the HOMO $3\sigma_u$ to the LUMO $4\sigma_g$ (Figure 1(a)), the energy gaps Δ_{01} between this state and the ground one, $^1\Sigma_g$, varies in the range of 10–13 eV, depending on the F-F distance.

Table 1
The values of imaginary frequencies ω (cm^{-1}), the height h (eV) and the width $2Q_{\min}$ (Å) of the energy barrier.

$R_{\text{F-F}}$ (Å)	ω	h	Q_{\min}
2.24	-	-	0.00
2.44	486.68	0.044	0.20
2.64	1333.84	0.340	0.35
2.84	1523.78	0.759	0.50

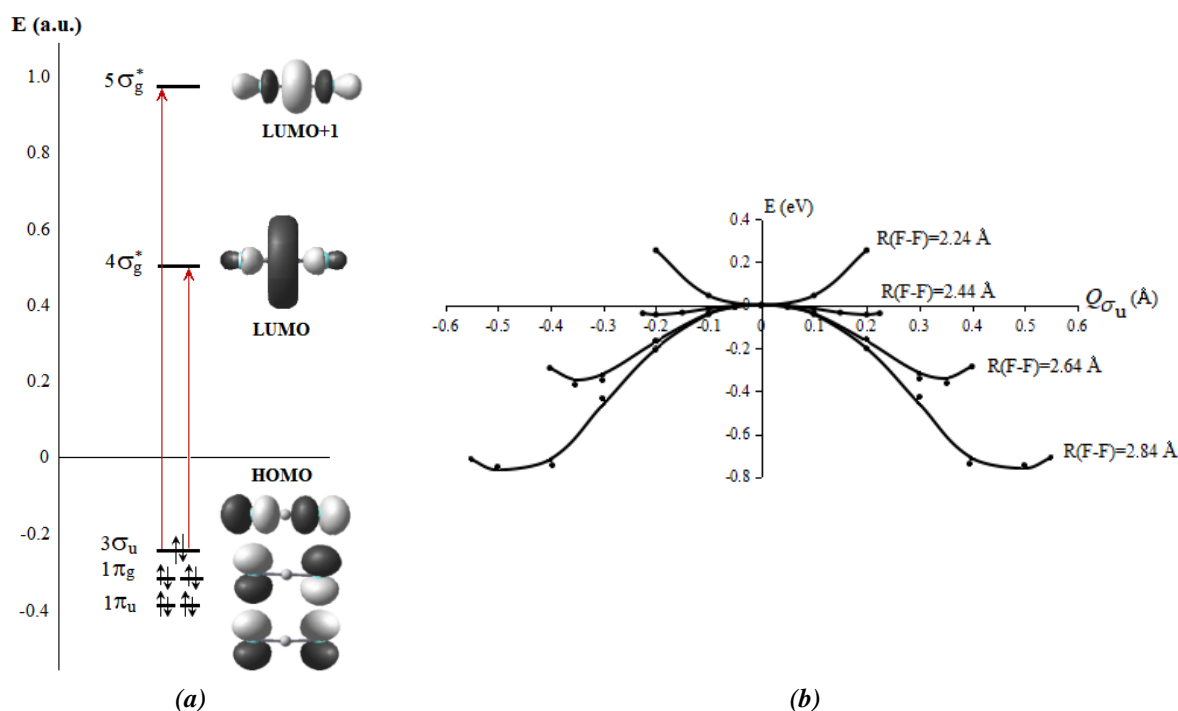


Figure 1. The MO energy level scheme for the $[\text{FHF}]^-$ molecules in the ground $^1\Sigma_g$ state with indication of the one-electron excitations to the $^1\Sigma_u$ terms (a); cross sections of the APES of $[\text{FHF}]^-$ along the σ_u -type distortion for several distances F...F (b); both *ab initio* and analytical (by Eq.(6)) calculations are shown by points and curves, respectively.

The second excited state, $2^1\Sigma_u$, with Δ_{02} more than 20 eV is formed by excitation HOMO \rightarrow LUMO+1. Subsequent higher-in-energy $1^1\Sigma_u$ excited states can be formed by one-electron excitations $1\pi_g\rightarrow 2\pi_u$, $1\pi_u\rightarrow 2\pi_g$, etc. If one can assume that the main contribution to the instability of the ground state comes from only the first excited state $1^1\Sigma_u$, then the PJTE problem is simplified to a two-level one, $(1^1\Sigma_g + 1^1\Sigma_u)\otimes\sigma_u$. The possible contribution of the second and all other higher lying excited $1^1\Sigma_u$ states to the curvature of the adiabatic potential of the ground state can be taken into account using the second-order corrections $-p_1$, as described in the previous Section, Eq.(5). If the value of $(K_{01}-p_1)$ in Eq.(6) is positive, this means that the higher excited states by themselves do not produce the instability of the ground state, and the lowest excited state $1^1\Sigma_u$ is responsible for the main contribution to its instability.

To estimate the parameters of the vibronic coupling between the ground $1^1\Sigma_g$ and the excited $1^1\Sigma_u$ states, *ab initio* calculations of the energy profiles (APES cross sections) of the systems along the coordinate of instability σ_u were performed. Results for several distances F \cdots F are shown in Figure 1(b).

It can be seen that at equilibrium R_{F-F} equals to 2.24 Å, the adiabatic potential is a single-well one, that is, the proton is located in the

middle between the fluorine atoms. Three lower curves in Figure 1(b) are the cuts of the APESes for $R_{F-F}= 2.44$ Å, $R_{F-F}= 2.64$ Å, and $R_{F-F}= 2.84$ Å, respectively. As the Q_{σ_u} coordinate, it was used the proton displacement from the center of the F-F distance. It is seen that, with increasing F-F distances, the symmetric $D_{\infty h}$ nuclear configuration becomes unstable with respect to the displacement of the central proton to one of the fluorine atoms, and the APESes become the double-well ones. The height and width of the energy barrier to the asymmetric displacement of the proton also increase.

By fitting Eq.(6) to the *ab initio* calculated energy profiles, we get the values of the PJTE parameter presented in Table 1. The parameters are as follows: the energy gaps Δ between the ground $1^1\Sigma_g$ and the excited $1^1\Sigma_u$ terms, the primary force constants $K_{01}-p_1$ and $K_{02}-p_2$ in them, the vibronic coupling constants F_{12} , and the resulting values of the curvature of the ground state APES, K_{gr} , which at small Q can be approximately estimated according Eq.(7). It is important to note that the obtained value of $K_{01}-p_1$ from Table 2 is positive, showing that vibronic mixing of the ground state with higher-lying excited states does not produce the instability of the ground state, and it is the first excited state $1^1\Sigma_u$ that is responsible for the main contribution to the instability.

Table 2

PJTE coupling constants F_{12} (eV/Å), energy gaps Δ (eV), primary force constants $K_{01}-p_1$ and $K_{02}-p_2$, and resulting force constants K_{gr} (in eV/Å²) in the reference $D_{\infty h}$ configuration of [FHF]⁻ anions obtained by fitting Eq. (6) to the *ab initio* calculated energy profiles.

R_{F-F} (Å)	Δ	F_{12}	$K_{01}-p_1$	$K_{02}-p_2$	K_{gr}
2.24	13.055	-	-	-	9.172
2.44	12.796	16.193	36.541	52.259	-4.443
2.64	11.826	15.980	30.847	32.796	-12.339
2.84	10.570	13.956	21.782	21.848	-15.073

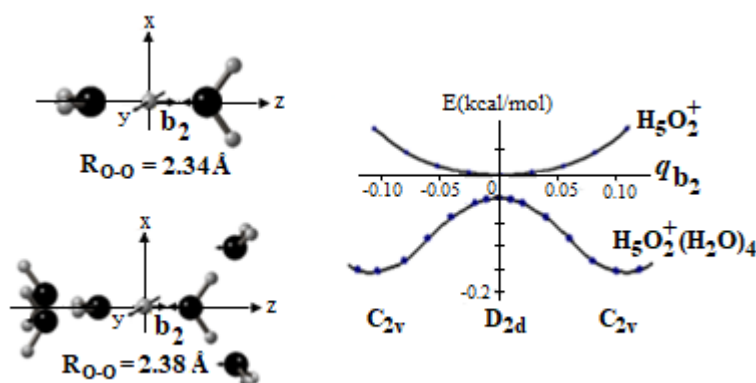


Figure 2. The cross sections of the APES along the off-center b_2 -type distortions for the Zundel cation $H_5O_2^+$ and for the $H_5O_2^+(H_2O)_4$ cluster.

It is also seen that the absolute value of the curvature of the adiabatic potential K_{gr} increases with increasing distance $F\cdots F$, which results in an increase in the height and width of the energy barrier (Table 1).

A similar effect was obtained by us earlier for dihydronium cation $H_5O_2^+$ [19]. As in the case of the $[FHF]^-$ anion, at the equilibrium O-O distance ($R_{O-O} = 2.34 \text{ \AA}$), the shared proton is located midway between the oxygen atoms (the single-well adiabatic potential in Figure 2). However, taking into account only the first solvation sphere around the Zundel cation in the $H_5O_2^+(H_2O)_4$ cluster leads to a double-well adiabatic potential energy surface along the hydrogen bond coordinate and to the instability of the central position of the proton. The R_{O-O} distance in this case is equal to 2.38 \AA (Figure 2).

Conclusions

In this work, using the $[FHF]^-$ system as an example, it has been shown that the hydrogen bonds in hydrogen bihalides $[XHX]^-$ can be described in the framework of the pseudo Jahn-Teller effect; all calculated potential energy curves along the off-center proton displacements wholly coincide with those predicted from the general vibronic theory. Thus, the functional dependence of the potential energy on the instability coordinate $\varepsilon(Q_{ou})$ following from the PJTE theory, with the parameters estimated using quantum chemical calculations, can serve as a parametrized analytical model of the adiabatic potential, which can be used to simulate the proton transfer process in such systems.

Calculations confirm also that the breathing mode that controls the F-F distance between two fluorine atoms plays a very important role in the proton transfer dynamics in such systems. While at the equilibrium F-F distance the shared proton is located midway between both fluorine atoms, its central position becomes unstable with increasing F-F distance. This instability is shown to originate due to the pseudo Jahn-Teller mixing of the ground electronic state $1^1\Sigma_g^-$ with the first excited state of $1^1\Sigma_u$ symmetry through the asymmetric σ_u vibrational mode.

Acknowledgments

This work was carried out within the project No. 20.80009.5007.27 "Physicochemical mechanisms of redox processes with electron transfer involved in vital, technological and environmental systems" supported by the National Agency for Research and Development (ANCD) of the Republic of Moldova.

References

- Chen, Ch.; Shi, T.; Chang, W.; Zhao, J. Essential roles of proton transfer in photocatalytic redox reactions. *ChemCatChem*. The European Society Journal for Catalysis, 2015, 7(5), pp. 724-731. DOI: <https://dx.doi.org/10.1002/cctc.201402880>
- Elliott, J.A.; Paddison, S.J. Modelling of morphology and proton transport in PFSA membranes. *Physical Chemistry Chemical Physics*, 2007, 9(21), pp. 2602-2618. DOI: <https://doi.org/10.1039/b701234a>
- Tommos, C. Electron, proton and hydrogen-atom transfers in photosynthetic water oxidation. *Philosophical Transactions of the Royal Society B: Biological Science*, 2002, 357(1426), pp. 1383-1394. DOI: <https://doi.org/10.1098/rstb.2002.1135>
- Petersen, M.K.; Voth, G.A. Characterization of the solvation and transport of the hydrated proton in the perfluorosulfonic acid membrane nafion. *The Journal of Physical Chemistry B*, 2006, 110(37), pp. 18594-18600. DOI: <https://doi.org/10.1021/jp062719k>
- Calio, P.B.; Li, Ch.; Voth, G.A. Molecular origins of the barriers to proton transport in acidic aqueous solutions. *The Journal of Physical Chemistry B*, 2020, 124(40), pp. 8868-8876. DOI: <https://dx.doi.org/10.1021/acs.jpcc.0c06223>
- Swanson, J.M.J.; Maupin, C.M.; Chen, H.; Petersen, M.K.; Xu, J.; Wu, Yu.; Voth, G.A. Proton solvation and transport in aqueous and biomolecular systems: Insights from computer simulations. *The Journal of Physical Chemistry B*, 2007, 111(17), pp. 4300-4314. DOI: <https://dx.doi.org/10.1021/jp070104x>
- Tanner, Ch.; Manca, C.; Leutwyler, S. Probing the threshold to H atom transfer along a hydrogen-bonded ammonia wire. *Science*, 2003, 302(5651), pp. 1736-1739. DOI: [10.1126/science.1091708](https://doi.org/10.1126/science.1091708)
- Grabowski, S.J. $[FHF]^-$ – The strongest hydrogen bond under the influence of external interactions. *Crystals*, 2016, 6(1), 3, pp. 1-17. DOI: <https://doi.org/10.3390/cryst6010003>
- Pylaeva, S.A.; Elgabarty, H.; Sebastiani, D.; Tolstoy, P.M. Symmetry and dynamics of FHF^- anion in vacuum, in CD_2Cl_2 and in CCl_4 . *Ab initio* MD study of fluctuating solvent-solute hydrogen and halogen bonds. *Physical Chemistry Chemical Physics*, 2017, 19(38), pp. 26107-26120. DOI: <https://doi.org/10.1039/C7CP04493C>
- Panich, A.M. NMR study of the F-H \cdots F hydrogen bond. Relation between hydrogen atom position and F-H \cdots F bond length. *Chemical Physics*, 1995, 196(3), pp. 511-519. DOI: [https://doi.org/10.1016/0301-0104\(95\)00128-B](https://doi.org/10.1016/0301-0104(95)00128-B)
- Cornaton, Y.; Marquardt, R. A global analytical representation of the potential energy surface of the FHF^- anion. *The Journal of Physical Chemistry A*, 2016, 120(30), pp. 5959-5968. DOI: <https://doi.org/10.1021/acs.jpca.6b05325>

12. Epa, V.C.; Choi, J.H.; Klobukowski, M.; Thorson, W.R. Vibrational dynamics of the bifluoride ion. I. Construction of a model potential surface. *The Journal of Chemical Physics*, 1990, 92(1), pp. 466-472.
DOI: <https://doi.org/10.1063/1.458449>
13. Denisov, G.D.; Mavri, J.; Sobczyk, L. Potential energy shape for the proton motion in hydrogen bonds reflected in infrared and NMR spectra. Grabowski, S.J. (Ed.) *Hydrogen Bonding-New Insights*. Springer: Dordrecht, The Netherlands, 2006, pp. 377-416. DOI: https://doi.org/10.1007/978-1-4020-4853-1_10
14. Bersuker, I.B. *The Jahn-Teller Effect*. Cambridge University Press, Cambridge UK, 2006, 616 p. DOI: <https://doi.org/10.1017/CBO9780511524769>
15. Bersuker, I.B. Jahn-Teller and Pseudo-Jahn-Teller Effects: From particular features to general tools in exploring molecular and solid state properties. *Chemical Reviews*, 2021, 121(3), pp. 1463-1512.
DOI: <https://doi.org/10.1021/acs.chemrev.0c00718>
16. Bersuker, I.B. Manipulation of structure and properties of two-dimensional systems employing the pseudo Jahn-Teller effect. *FlatChem*, 2017, 6, pp. 11-27.
DOI: <https://doi.org/10.1016/j.flatc.2017.10.001>
17. Gorinchoy, N. Pseudo Jahn-Teller Effect in puckering and planarization of heterocyclic compounds. *International Journal of Organic Chemistry*, 2018, 8(1), pp. 142-159.
DOI: <https://doi.org/10.4236/ijoc.2018.81010>
18. García-Fernández, P.; García-Canales, L.; García-Lastra, J.M.; Junquera, J.; Moreno, M.; Aramburu, J.A. Pseudo-Jahn-Teller origin of the low barrier hydrogen bond in $N_2H_7^+$. *The Journal of Chemical Physics*, 2008, 129(12), 124313, pp. 1-14.
DOI: <https://doi.org/10.1063/1.2980053>
19. Geru, I.I.; Gorinchoy, N.N.; Balan, I.I. Pseudo Jahn-Teller origin of the proton tunneling in Zundel cation containing water clusters. *Ukrainian Journal of Physics*, 2012, 57(11), pp. 1149-1155.
http://nbuv.gov.ua/UJRN/Ukjourph_2012_57_11_9
20. Bersuker, I.B.; Gorinchoy, N.N.; Polinger, V.Z. On the origin of dynamic instability of molecular systems. *Theoretica Chimica Acta*, 1984, 66, pp. 161-172.
DOI: <https://doi.org/10.1007/BF00549666>
21. Bersuker, I.B.; Gorinchoy, N.N.; Polinger, V.Z. Pseudo Jahn-Teller origin of square-planar configuration instability of main-group element hydrides. *Journal of Molecular Structure*, 1992, 270, pp. 369-380. DOI: [https://doi.org/10.1016/0022-2860\(92\)85040-N](https://doi.org/10.1016/0022-2860(92)85040-N)
22. Gorinchoy, N.N.; Cimpoesu, F.; Bersuker, I.B. A comparative study of the pseudo Jahn-Teller instability of linear molecules Ag_3 and I_3 and their positive and negative ions. *Journal of Molecular Structure (THEOCHEM)*, 2001, 530(3), pp. 281-290. DOI: [https://doi.org/10.1016/S0166-1280\(99\)00497-2](https://doi.org/10.1016/S0166-1280(99)00497-2)
23. Liu, Y.; Bersuker, I.B.; Zou, W.; Boggs, J.E. Pseudo Jahn-Teller versus Renner-Teller Effects in the instability of linear molecules. *Chemical Physics*, 2010, 376(1-3), pp. 30-35. DOI: <https://doi.org/10.1016/j.chemphys.2010.07.029>
24. Hermoso, W.; Ilkhani, A.R.; Bersuker, I.B. Pseudo Jahn-Teller origin of instability of planar configurations of hexa-heterocycles $C_4N_2H_4X_2$ (X= H, F, Cl, Br). *Computational and Theoretical Chemistry*, 2014, 1049, pp. 109-114.
DOI: <https://doi.org/10.1016/j.comptc.2014.10.007>
25. Ilkhani, A.R.; Hermoso, W.; Bersuker, I.B. Pseudo Jahn-Teller origin of instability of planar configurations of hexa-heterocycles. Application to compounds with 1,2- and 1,4- C_4X_2 skeletons (X= O, S, Se, Te). *Chemical Physics*, 2015, 460, pp. 75-82. DOI: <https://doi.org/10.1016/j.chemphys.2015.02.017>
26. Hehre, W.J.; Ditchfield, R.; Pople, J.A. Self-Consistent Molecular Orbital Methods. XII. Further extensions of Gaussian-type basis sets for use in molecular orbital studies of organic molecules. *The Journal of Chemical Physics*, 1972, 56(5), pp. 2257-2261.
DOI: <https://doi.org/10.1063/1.1677527>
27. Granovsky, A.A. GAMESSm- computational chemistry program.
<http://classic.chem.msu.su/gran/gamess/index.html>
28. Schmidt, M.W.; Baldrige, K.K.; Boatz, J.A.; Elbert, S.T.; Gordon, M.S.; Jensen, J.H.; Koseki, S.; Matsunaga, N.; Nguyen, K.A.; Su, S.; Windus, T.L.; Dupuis, M.; Montgomery Jr, J.A. General atomic and molecular electronic structure system. *Journal of Computational Chemistry*, 1993, 14(11), pp. 1347-1363.
DOI: <https://doi.org/10.1002/jcc.540141112>